

# Performance of SIMO FM-DCSK UWB System Based on Chaotic Pulse Cluster Signals

Lin Wang, *Senior Member, IEEE*, Xin Min, and Guanrong Chen, *Fellow, IEEE*

**Abstract**—Recently, an ultra-wideband (UWB) system with frequency-modulated differential chaos shift keying (FM-DCSK) modulation has attracted increasing interest for its many distinctive superiorities over its conventional counterparts, especially in low-rate and low-power wireless personal area network (WPAN) applications. However, some of its drawbacks, such as low energy efficiency, complex implementation and weak multiaccess capacity, have also been noticed, which restrict its further acceptance and applications. To overcome these problems, an architecture, named single-input and multiple-output (SIMO) FM-DCSK UWB system, is introduced in this paper. With chaotic transmitted signals based on a high-order Walsh function and multiple antennas diversity reception, this paper demonstrates the superiorities of the new system in bit error rate (BER) performance as well as in moderation complexity. Furthermore, by transmitting chaotic pulse cluster signals, an improved emission signal structure of the SIMO FM-DCSK UWB system is proposed so as to overcome the delay line implementation constraints and to further enhance the BER performance. Based on this new signal format, a method of combining time division and Walsh function division is introduced into the existing Walsh function division scheme, thereby resolving the inherent obstacle in user capability which was known to be limited by the order of the Walsh function.

**Index Terms**—Chaotic pulse cluster, frequency-modulated differential chaos shift keying (FM-DCSK), single-input multiple-output (SIMO), ultra-wideband (UWB).

## I. INTRODUCTION

ULTRA-WIDEBAND (UWB) transmission technology has received great attention in both academia and industry for its promising potentials and applications in wireless communications, especially in wireless personal area networks (WPANs). A UWB signal has a wide bandwidth, which can be extended from 3.1 GHz up to 10.6 GHz today, with a low power spectrum density. However, it must be controlled to satisfy the

Manuscript received May 26, 2010; revised November 08, 2010; accepted January 07, 2011. This work was supported by the NSF in Fujian Province (No. 2008J0035) and NSF of China (Nos. 60972053, 61001073, and 10832006), as well as the Hong Kong Research Grants Council (No. CityU1117/10E). This work was presented in part at the 9th International Symposium on Communication and Information Technology (ISCIT 2009), Incheon, Korea, Sep. 2009. This paper was recommended by Associate Editor G. Sobelman.

L. Wang is with the Department of Communication Engineering, Xiamen University, Fujian 361005, China (e-mail: wanglin@xmu.edu.cn).

X. Min is with the Department of Wireless Networks Performance Research, Huawei Company, Chengdu 610041, China (e-mail: xinmin225@gmail.com).

G. Chen is with the Department of Electronic Engineering, City University of Hong Kong, Hong Kong SAR, China (e-mail: gchen@ee.cityu.edu.hk).

Color versions of one or more of the figures in this paper are available online at <http://ieeexplore.ieee.org>.

Digital Object Identifier 10.1109/TCSI.2011.2112592

Federal Communications Commission (FCC) regulations [2] in order not to interfere the traditional narrow-band systems sharing the same frequency band. (It is noted that neither the type of carrier nor the modulation technique is defined in the FCC regulations.) Thus, it provides a new solution to reuse the assigned frequency.

As one type of wideband carriers, chaotic signals can be generated by simple circuits in any frequency band and at arbitrary power level [3]–[6]. Mapping digital information to chaotic signals, one can implement spread spectrum (SS) systems since the bandwidth of a transmitted chaotic signal is much larger than the data rate. Besides, the spectrum of a chaotic signal is inherently wide, which will not change even if the chaotic pulse width is altered [7]. Combining the emerging technologies with UWB transmission, a “UWB Direct Chaotic Communication (UWB-DCC) System” was proposed to respond to the IEEE 802.15.4a call for proposals in 2005 [8], where chaotic pulse was accepted as a candidate waveform in this formal IEEE standard [9].

Among all the chaotic modulation schemes that can be used in the UWB-DCC system [4], [10], [11], the FM-DCSK scheme is proven not only having the best noise performance but also achieving an excellent anti-multipath fading capability [10]–[14]. Meanwhile, space diversity as well as increasing data rate can be achieved by the FM-DCSK scheme based on the SIMO architecture [15]. As a result, it has been considered as an alternative of the UWB-DCC system in the literature [16]–[20]. Specifically, in [16], [17], Kolumbán was the first to determine the feasibility of an FM-DCSK UWB radio system and give an exact expression for the noise performance of the generalized transmitted reference (TR) system with a comparison between the FM-DCSK and the noncoherent impulse radio systems. The authors of [18] discussed several key features and the principle of operation of FM-DCSK in combination with the UWB technology. Important system parameters were analyzed and optimized in [19], which demonstrated its promising advantages in indoor communication systems. Recently, a data-aided timing synchronization algorithm was proposed for the FM-DCSK UWB system to resolve technical challenges regarding the receiver implementation [20].

However, some drawbacks of the FM-DCSK UWB system have been noticed, which restrict its further applications, including the following: i) Performing differential correlation detection based on the transmitted reference (TR) system [21] wastes one half of the signal power to transmit the noninformation-bearing reference pulse. Moreover, the correlation detection template is disturbed by noise; thus it has a somewhat worse performance. ii) Ultra high sampling frequency makes the

digital implementation of the FM-DCSK UWB system almost impossible, whereas the requirement of wideband delay lines is also a great challenge for its analog implementation. The chaotic signal is noncyclic, so both transmitter and receiver of the original FM-DCSK UWB system need semi-bit-long delay lines. iii) Nonorthogonal of finite length chaotic signals and complex implementation of orthogonal high-order Walsh functions imply that the existing DCSK/FM-DCSK-based multiaccess scheme is infeasible or inefficient in UWB applications [22]. Therefore, multiaccess solution becomes an important issue for the FM-DCSK UWB system, especially in low-power and low-cost applications.

To resolve the aforementioned technical problems, a new SIMO FM-DCSK UWB system was introduced in [23]. Comparing to the original SIMO FM-DCSK architecture presented in [15], not a single substream but multistream signals are transmitted herein, so as to well cope with the low-rate UWB applications. In this case, simple differential correlation detection as well as generalized maximum likelihood detection can be performed at the receiver side. In fact, its performance has been studied under the IEEE 802.15.4a application environment in [23], showing that higher energy efficiency and lower moderation implementation complexity, as well as relatively low delay lines, can be achieved as compared with the original FM-DCSK UWB system [19].

Noticeably, implementing wideband delay lines still remains a great challenge for the SIMO FM-DCSK UWB system introduced in [23]. In this paper, a novel transmitted signal structure named chaotic pulse cluster is proposed to resolve this technical problem. In the new enhanced version, the space between the adjacent pulses within the same symbol duration is fixed; therefore, it is no longer being affected by the order of the Walsh function but can be further reduced to an acceptable range of delay lines. Concentrating all chaotic pulses within a small portion of the bit duration to perform pulse cluster transmission, it becomes a general UWB signal format with a narrow pulse duration, low duty cycle and long guard interval, thus significantly improving system performances under the UWB transmission environment. Incidentally, this signal structure provides a desirable solution to the Walsh function division scheme presented in [24] but for multiusers communication systems. Separating both in time and in the Walsh function domain, the problem of user capability being limited by the order of the Walsh function can be avoided, which greatly enhance the multiaccess capability thereby resolving the multiaccess issue of the FM-DCSK UWB system fairly effectively.

The rest of this paper is organized as follows. Section II describes some basic principles of the SIMO FM-DCSK UWB system. Its enhanced version is discussed in Section III. Section IV presents a multiaccess solution based on the new signal structure. Simulation results and analysis are then given in Section V. Finally, Section V concludes the paper.

## II. BASIC PRINCIPLES OF THE SIMO FM-DCSK UWB SYSTEM

First, recall that FM-DCSK uses a frequency-modulated chaotic signal as the carrier, with a DCSK modulator, for transmission [14]. A chaotic signal is generated by a chaotic

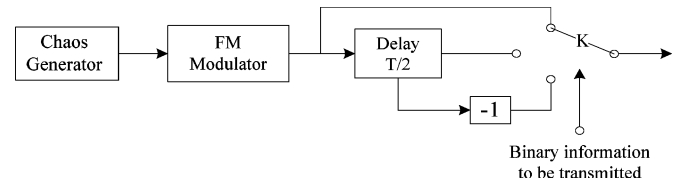


Fig. 1. Binary FM-DCSK modulator.

mapping method, while the simple cubic chaotic map is chosen here for implementation. Together with a binary FM-DCSK modulator, the setting is illustrated in Fig. 1.

The binary FM-DCSK modulation unit transmits a reference segment of the frequency-modulated chaotic signal, or its repeated or reverse segment, according to the digital information “1” or “0,” respectively. The modulated signal is represented by two orthogonal basic functions,  $g_1(t)$  and  $g_2(t)$ , as follows:

$$\begin{aligned} s_m(t) &= s_{m1}g_1(t) + s_{m2}g_2(t) \\ (s_{11} \quad s_{12}) &= (\sqrt{E_b} \quad 0) \\ (s_{21} \quad s_{22}) &= (0 \quad \sqrt{E_b}) \end{aligned} \quad (1)$$

where  $s_m(t)$  is the modulated signal for transmission and  $E_b$  is the bit energy. The two basic orthogonal functions are

$$\begin{aligned} g_1(t) &= \begin{cases} +c(t), & 0 \leq t < T/2 \\ +c(t - T/2), & T/2 \leq t < T \end{cases} \\ g_2(t) &= \begin{cases} +c(t), & 0 \leq t < T/2 \\ -c(t - T/2), & T/2 \leq t < T. \end{cases} \end{aligned} \quad (2)$$

Here,  $T$  is the bit duration,  $c(t)$  is the frequency-modulated chaotic carrier, with bit energy being normalized to one, and the differential modulating process follows the second-order Walsh functions

$$W_2 = \begin{bmatrix} w_1 \\ w_2 \end{bmatrix} = \begin{bmatrix} +1 & +1 \\ +1 & -1 \end{bmatrix}. \quad (3)$$

The two row vectors  $w_1$  and  $w_2$  are multiplied with the carrier segment as the weights when the digital information is “1” or “0,” respectively. Higher order Walsh functions will be used for dividing multiple substreams, as further discussed in the next section.

### A. Transmitter

In the proposed SIMO FM-DCSK UWB system, a higher order Walsh function is adopted in the transmitter. Unlike the second-order Walsh scheme in the original FM-DCSK UWB system [19], a higher order Walsh function has more than two row vectors. For example, with the order number  $M = 4$ , the fourth-order Walsh function has four row vectors. However, differing from in the existing SIMO FM-DCSK system which uses all the row vectors of the higher order Walsh function to achieve multiple substreams transmission [15], only the first two rows (i.e.,  $w_1$  and  $w_2$ ) are assigned to form single substream transmission in the proposed SIMO FM-DCSK UWB system. Represented by the two basis functions  $g_1(t)$  and  $g_2(t)$ , four pulses (i.e.,  $c_0(t)$ ,  $c_1(t)$ ,  $c_2(t)$ ,  $c_3(t)$ ) will be transmitted for one information bit in this scenario. Here,  $T_c$  is the duration of the single

pulse and  $T$  is the bit duration. And the amounts of pulses will be further increased with the Walsh function order,  $M$ .

Considering bit energy constant, the amplitude of each pulse is lowered to accord with the low-power spectrum required by the Federal Communications Commission (FCC) regulation in the proposed scheme

$$W_4 = \begin{bmatrix} w_1 \\ w_2 \\ w_3 \\ w_4 \end{bmatrix} = \begin{bmatrix} +1 & +1 & +1 & +1 \\ +1 & -1 & +1 & -1 \\ +1 & +1 & -1 & -1 \\ +1 & -1 & -1 & +1 \end{bmatrix} \quad (4)$$

$$g_1(t) = \begin{cases} +c_0(t), & 0 < t \leq T_c \\ +c_1(t), & T/4 < t \leq T/4 + T_c \\ +c_2(t), & T/2 < t \leq T/2 + T_c \\ +c_3(t), & 3T/4 < t \leq 3T/4 + T_c \end{cases} \quad (5)$$

$$g_2(t) = \begin{cases} +c_0(t), & 0 < t \leq T_c \\ -c_1(t), & T/4 < t \leq T/4 + T_c \\ +c_2(t), & T/2 < t \leq T/2 + T_c \\ -c_3(t), & 3T/4 < t \leq 3T/4 + T_c \end{cases} \quad (5)$$

$$c_1(t) = c_0(t - T/4)$$

$$c_2(t) = c_0(t - T/2)$$

$$c_3(t) = c_0(t - 3T/4). \quad (6)$$

It is particularly worth noting that the carriers in the FM-DCSK modulation scheme here are continuously varying chaotic waveforms, i.e., the chaotic carriers  $c(t)$  are not the same in different symbols. Therefore, they will also be different in different chips of the same symbol if having no necessary measures. To ensure the same chaotic carriers in all chips of the same symbol shown in (6), a series of delay lines are needed in the transmitter of the higher order Walsh scheme, where the unit delay is  $T/M$ , decreasing with the order  $M$  of the Walsh function.

### B. Receiver

Regarding the detection scheme in the receiver of the SIMO FM-DCSK UWB system, the differential correlation (DC) detection is performed in the existing FM-DCSK UWB system [19], whereas the generalized maximum likelihood (GML) detection is adopted in the existing SIMO FM-DCSK system [15]. Since combining the higher order Walsh scheme with single substream transmission, the above two detections both can be used in the proposed system. The two block diagrams of the two receiver schemes are shown in Figs. 2 and 3, respectively. Note that the problem of time symbol synchronization is assumed herein, because it has already been discussed and solved in [20].

In Fig. 2, differential correlation detection is performed in each antenna, and then the decision vectors are combined in an equal gain way. With  $N$  antennas, it is expressed as in (7). Here,  $T$  is the bit duration,  $r_n(t)$  is the received signal in receiver antenna  $n$ , and  $M$  is the order of the adopted Walsh function. The estimated bit will be “1” if the total decision vectors  $E_{DC} > 0$ , or “0” if  $E_{DC} \leq 0$ . Here,

$$E_{DC} = \sum_{n=1}^N \int_{T/M}^T r_n(t)r_n(t - T/M)dt. \quad (7)$$

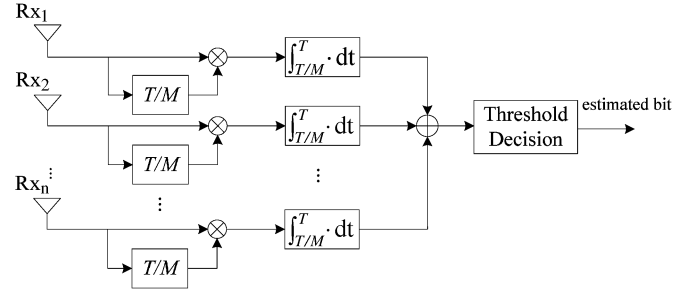


Fig. 2. Block diagram of differential correlation (DC) detection.

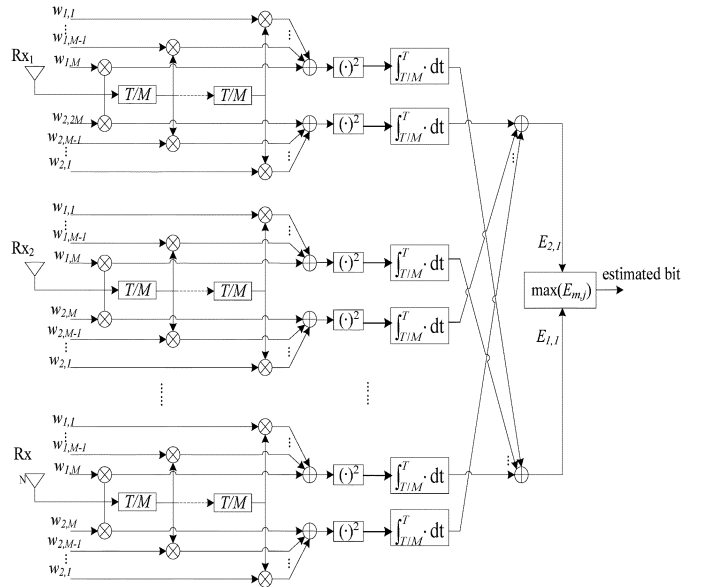


Fig. 3. Block diagram of generalized maximum likelihood (GML) detection.

In [25], the Fourier analyzer concept was introduced to describe the detection problem in chaotic communications. Based on the Fourier coefficients, a classification of detection techniques was given. The key issue in detection is the maximization of the signal-to-noise ratio in the observation variable, and *a priori* knowledge on the Fourier series coefficients of the basis functions has to be used to suppress the noise effects. The Fourier analyzer concept has been used to develop some new detector configurations for the FM-DCSK modulation scheme [26].

Fig. 3 shows the GML detection scheme. The detection process is carried out through each receiver antenna independently, with the corresponding Walsh functions (i.e.,  $w_1$  and  $w_2$ ) used in the transmitter. Then, the weighted energy calculated from each receiver antenna is combined for final decision-making. The weighted energy combined with antennas can be expressed as

$$E_{GML} = \sum_{n=1}^N \int_{T/M}^T \left[ \sum_{i=0}^{M-1} r_n \left( t - i \frac{T}{M} \right) \cdot w_{1,M-i} \right]^2 dt - \sum_{n=1}^N \int_{T/M}^T \left[ \sum_{i=0}^{M-1} r_n \left( t - i \frac{T}{M} \right) \cdot w_{2,M-i} \right]^2 dt. \quad (8)$$

Here,  $r_n(t - iT/M)$  is the received signal in receiver antenna  $n$  which has delay  $iT/M$ . Using vector  $w_1$  for bit “1” and vector

TABLE I  
DELAY REQUIREMENTS OF DC AND GML DETECTIONS

	DC detection	GML detection
Unit delay	$T/M$	$T/M$
Block amount	$N$	$N \times (M-1)$
Total delay	$T \times N/M$	$T \times N \times (M-1)/M$

TABLE II  
UNIT DELAY REQUIREMENTS FOR THE PROPOSED SYSTEM  
WITH DIFFERENT VALUES OF  $M$

$M$	Unit delay (ns)
4	250
8	125
16	62.5
32	31.25
64	15.625

$w_2$  for bit “0,” the decision will be “1” if the total decision vectors  $E_{GML} > 0$ , or “0” if  $E_{GML} \leq 0$ .

The delay requirements of two receiver schemes are given in Table I, which demonstrates that the amounts of the DC detection (i.e.,  $N$ ) are less than the GML detection (i.e.,  $N \times (M-1)$ ), due to the higher order Walsh function ( $M > 2$ ) used in the proposed system. As all the delays of each block (the unit delay) are equal to  $T/M$ , the DC detection scheme is relatively easier to implement. Meanwhile, the unit delay  $T/M$  depends on the order  $M$  of the Walsh function when the bit duration  $T$  or the data rate  $R$  is constant. Usually, the requirements of unit delay are lowered with the increase of  $M$ . If so, the amounts of the delay blocks are increased in the GML detection scheme, a cost to pay for implementation. In other words, the complexity of the proposed system based on GML detection is increased with  $M$ . Furthermore, BER performance and transmitter complexity are both affected by the order value  $M$ , no matter which detection scheme is performed. Therefore, the order  $M$  of the Walsh function is a considerably important system parameter, which will be further investigated through simulations in Section V.

### III. PRINCIPLES OF SIMO FM-DCSK UWB SYSTEM BASED ON CHAOTIC PULSE CLUSTER SIGNALS

In Table II, the unit delay requirements of the proposed SIMO system with different Walsh function orders  $M$  are given. It can be seen that the unit delay is decreased with the increasing of  $M$  when the bit duration  $T$  is constant, which is set to be  $1 \mu\text{s}$  corresponding to the IEEE 802.15.4a low-rate applications. As implementing tens of nanosecond delay lines is unacceptable by the existing technology [27], [28],  $M$  must be large enough in order to make the unit delay requirements realizable. But, the complexity may be increased with  $M$ , which will be too high to implement in general. Meanwhile, the BER performance is affected by  $M$ , as discussed in the previous section. Thus, the proposed SIMO FM-DCSK UWB system should be further improved, for which an improved version of the transmitted signal structure is developed and presented in this section, which will be called a pulse cluster signal former.

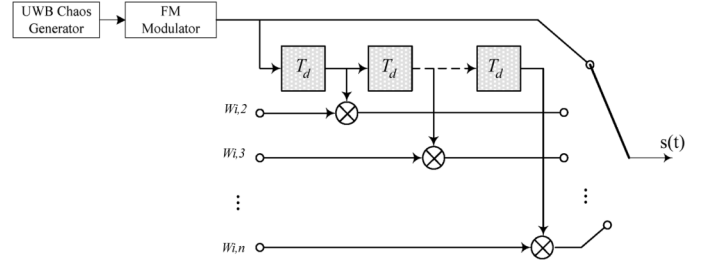


Fig. 4. Block diagram of the transmitter in the SIMO FM-DCSK UWB system based on chaotic pulse cluster signals.

In the pulse cluster version, the only difference is in the space between the adjacent pulses (i.e., the unit delay amount) within one symbol duration, as compared to the original system. It is no longer depending on the Walsh function order  $M$ , which can be fixed to a value defined by  $T_d$  and furthermore be reduced into an acceptable range of delay lines. It is worth noting that the improved transmitted signal format becomes a general UWB signal mode with a narrow pulse duration, low duty cycle and long guard interval, thereby making the proposed system corresponding well with the UWB communication applications.

As in the original SIMO system, the transmitted bits “1” or “0” are still represented by two basis functions in the improved version (i.e., pulse cluster signals version), but the positions of the chaotic pulses are changed. Taking  $M = 4$  as an example again, the emission time of the four pulses (i.e.,  $c_0^*(t)$ ,  $c_1^*(t)$ ,  $c_2^*(t)$ ,  $c_3^*(t)$ ) is compressed as shown in (9). Clearly, the unit delay amount in the transmitter is changed to  $T_d$  as in (10), whereas it was  $T/M$  in the original version as in (6). As seen in Fig. 4, the delay implementation of the chaotic pulse cluster signals is performed by a group of delay lines, whose unit delay is  $T_d$ . Here,

$$g_1^*(t) = \begin{cases} +c_0^*(t) & 0 < t \leq T_c \\ +c_1^*(t) & T_d < t \leq T_d + T_c \\ +c_2^*(t) & 2T_d < t \leq 2T_d + T_c \\ +c_3^*(t) & 3T_d < t \leq 3T_d + T_c \end{cases}$$

$$g_2^*(t) = \begin{cases} +c_0^*(t) & 0 < t \leq T_c \\ -c_1^*(t) & T_d < t \leq T_d + T_c \\ +c_2^*(t) & 2T_d < t \leq 2T_d + T_c \\ -c_3^*(t) & 3T_d < t \leq 3T_d + T_c \end{cases} \quad (9)$$

$$c_1^*(t) = c_0^*(t - T_d)$$

$$c_2^*(t) = c_0^*(t - 2T_d)$$

$$c_3^*(t) = c_0^*(t - 3T_d). \quad (10)$$

Comparing the DC and the GML detections, the receiver based on the DC detection has superior performance as well as relatively low complexity, as will be verified by simulations and analysis in Section V. Thus, only the DC detection is discussed for the single user case of the improved version. Its block diagram is described in Fig. 5, which is relatively simple and only  $T_d$  delay is demanded in each antenna.

In Fig. 6(a) and (b), the original and improved versions of the proposed system based on DC detection are shown. It may seem that the BER performance is deteriorated by more severe interpulse interference (IPI) in the improved version. However, this happens by contraries that the BER performance actually

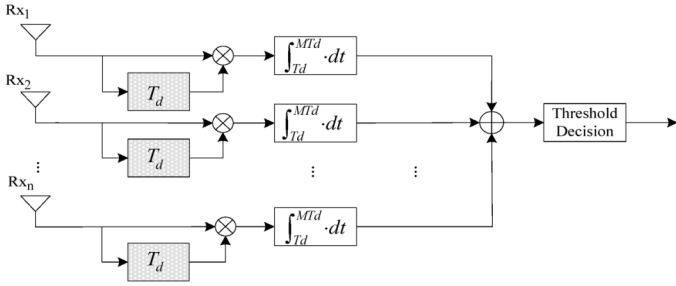


Fig. 5. Block diagram of the DC detection receiver in the SIMO FM-DCSK UWB system based on chaotic pulse cluster signals.

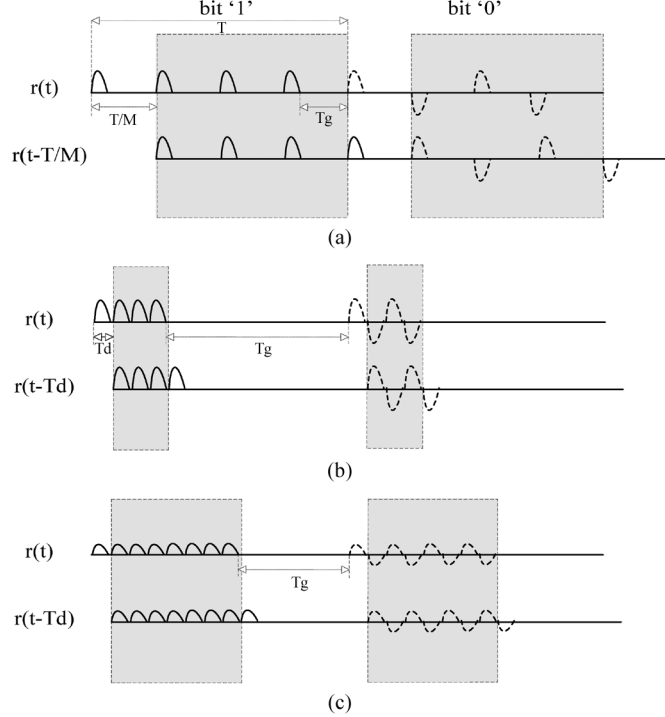


Fig. 6. Comparison between the original and improved versions of the proposed SIMO FM-DCSK UWB system based on DC detection. (a) Unimproved ( $M = 4$ ). (b) Improved ( $M = 4$ ). (c) Improved ( $M = 8$ ).

gets better, which will be confirmed by simulations in Section V. Three reasons are given here: i) Shorter integration interval (the shadow denotes) means less captured noise energy, while the collected signal energy is almost unchanged. ii) Longer guard time  $T_g$  between the adjacent symbols means less intersymbol interference (ISI). iii) For a certain length  $T_d$ , the effect of IPI is unobvious

$$E_c = (1 - 1/M)E_b. \quad (11)$$

Considering the influence of the Walsh function order value  $M$  in the improved version, a comparison between  $M = 4$  and  $M = 8$  is given in Fig. 6(b) and (c). It can be seen that the collected signal energy  $E_c$  is increased with  $M$  as clear from (11). In other words, the energy efficiency is improved with the increase of  $M$ . On the other hand, however, the energy of each pulse decreases with  $M$  increasing, which may become too small to against the noise effect. Besides, the integration interval gets longer with increasing value of  $M$ ; therefore, more noise energies are captured in the correlation integrator, which worsens

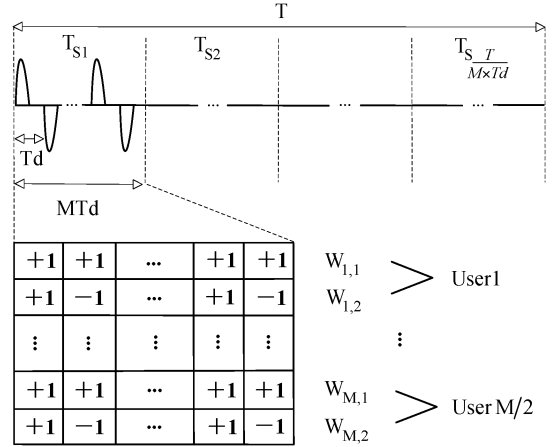


Fig. 7. The new multiaccess scheme.

the BER performance. Thus, similar to the original version,  $M$  is an important system parameter which can be optimized, and this will be further discussed through simulations in Section V.

#### IV. MULTIACCESS SCHEME OF THE PROPOSED UWB SYSTEM

Multiaccess communication is an important issue for the WPANs based on the proposed SIMO FM-DCSK UWB system. However, so far there are no publications discussing the multiaccess scheme for the FM-DCSK UWB system, although some multiaccess schemes have been studied and applied in the DCSK/FM-DCSK system over an AWGN channel [24], [29]–[31], or a multipath fading channel [32], [33]. Among all the existing schemes, the method of using orthogonal Walsh functions to separate different users has the best multiaccess performance [24], where, however, only  $M/2$  users can be accommodated if  $M$ -order Walsh function is used. Considering that the system complexity is increased with  $M$ , the problem of user capability restricting by the order of the Walsh function indeed limits its further applications.

In the pulse cluster version of the proposed SIMO FM-DCSK UWB system, the position of the pulse has been moved to the front of the bit duration, thus many empty signals remaining as shown in Fig. 6(b) and (c). The method of time division is introduced into the existing Walsh function division scheme here in a natural way. As shown in Fig. 7, the bit duration  $T$  is divided into several time slots  $T_s$ , totaling  $T/(M \times T_d)$ , which means that they can accommodate  $T/(M \times T_d)$  users in the time domain. Furthermore, within each time slot two different row vectors (e.g.,  $W_{1,1}$ ,  $W_{1,2}$ ) of  $M$  vectors in the higher order Walsh function can be assigned to each user. In this way, additional  $M/2$  users can access in each time slot thanks to the orthogonality of each row vector in the Walsh function. Here,

$$C_u = \frac{T}{M \times T_d} \times \frac{M}{2} = \frac{T}{2T_d}. \quad (12)$$

*Remark 1 (The User Capacity  $C_u$  No Longer Limited by  $M$ ):* As shown in (12), by combining the time division and the Walsh function division, the user capability  $C_u$  is increased to  $T/2T_d$  in the new scheme. Clearly, it has nothing to do with  $M$ , thus the implementation problem in the existing Walsh function division scheme is resolved effectively. However, by using more

than two row vectors of the Walsh function, not the DC detection but the GML detection could be adopted in the multiaccess scheme of the improved system. As a cost, the complexity is increased to a certain extent in the multiusers case. And it will have a tighter specification for the clock recovery circuit because all users must be synchronized at the symbol, just like in the existing Walsh function division scheme [24].

*Remark 2 (The User Capacity  $C_u$  Affected by  $T_d$ ):* The user capacity  $C_u$  equals to  $T/2T_d$ , which can be further increased by decreasing  $T_d$  even when the data rate  $R$  is fixed. As mentioned previously, decreasing  $T_d$  means lowering the delay lines requirements, which makes its implementation easier; while the performance would be deteriorated by severer IPI especially when  $T_d$  is very small. Thus, the user capacity  $C_u$  can be determined according to practical applications requirements.

*Remark 3 (The Data Rate  $R$  Altered for Different User):* Multiple substream signal transmission can be achieved for a certain user who has a higher data rate  $R$  demand by assigning more than two row vectors of a higher order Walsh function, similarly to the SIMO FM-DCSK scheme [15]. In other words, different data rate transmission requirements typically existing in WPAN can be reached in the new scheme while not disturbing the symbol synchronization among all users.

## V. SIMULATION RESULTS

In this section, simulation results of the proposed SIMO FM-DCSK UWB system and the new multiaccess scheme are presented with different system parameters (i.e., Walsh function orders  $M$ , receive antenna number  $N$ , and user number  $U$ ). As above, the general SIMO FM-DCSK UWB system is called the original version while the pulse cluster form is called the improved version. All the simulations are performed under the representative indoor channels, i.e., IEEE 802.15.4a CM1 channels [34], which is based on line-of-sight (LOS) indoor residential. The parameters are set as follows: bit duration  $T = 1 \mu\text{s}$ , chaotic pulse width  $T_c = 2.5 \text{ ns}$ , sampling frequency for simulation  $f_s = 8 \text{ GHz}$ , and the cubic chaotic map is chosen for chaos pulse generation.

### A. Comparison Between the Existing FM-DCSK UWB and the Proposed SIMO FM-DCSK UWB System Including the Original and Improved Versions

First, consider the single-user case on the BER performance of the existing FM-DCSK UWB. The proposed SIMO FM-DCSK UWB and its improved version are simulated in CM1. The system parameters are set as follows: the Walsh function order  $M = 2$  and the receiving antenna  $N = 1$  in the existing FM-DCSK UWB system;  $M = 4$  and  $N = 2$  in the proposed SIMO FM-DCSK UWB system with DC and GML detections;  $M = 4$ ,  $N = 2$  and  $T_d = 125 \text{ ns}$ ,  $62.5 \text{ ns}$ ,  $31.25 \text{ ns}$ ,  $15.625 \text{ ns}$ ,  $10 \text{ ns}$  in the improved version with DC detection. And the user number  $U = 1$  in all the simulations in this subsection.

In Fig. 8, it can be seen that the improved version of the proposed SIMO FM-DCSK UWB system has the best BER performance, its original version is second, but the existing FM-DCSK UWB scheme is the worst in general.

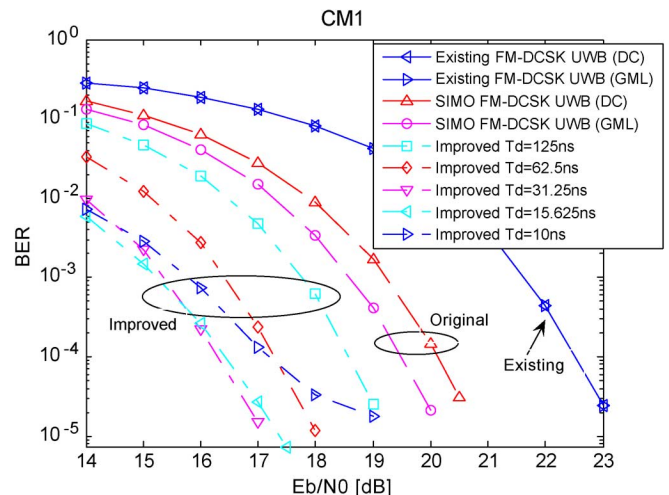


Fig. 8. BER performance comparison between the existing FM-DCSK UWB and the proposed SIMO FM-DCSK UWB system.

- (i) *Comparison between the DC and GML detection:* Note that in Fig. 8, the BER performance of the GML detection is equal to the DC detection in the existing FM-DCSK UWB system (i.e.,  $M = 2$ ). With  $M > 2$ , however, the GML detection is better than the DC detection in the original version of the proposed system due to the  $(M - 1)$  times addition operations which achieve denoising in the GML detection. However, as mentioned in Section II, it has much higher demands on delay lines and needs more complex implementation than the DC detection especially when  $M$  is large. In other words, the proposed system based on the GML detection is more complex and harder to implement in general. Accordingly, by trading off the performance and the complexity, the DC detection becomes the right choice for the proposed system in low-power applications. That is why DC detection is adopted in the improved version of the proposed system.
- (ii) *The effect of  $T_d$  on the BER performance:* As described in Section III, the BER performance of the improved version is affected by the unit delay  $T_d$ . Actually, the effect of  $T_d$  on the existing system and on the original version can also be analyzed, with  $T_d = 500 \text{ ns}$  in the former and  $T_d = 250 \text{ ns}$  in the latter. And the influence of  $T_d$  is embodied by means of altering the noise energy captured and by the IPI. At the beginning, the BER performance is greatly improved with the decreasing of  $T_d$ , i.e., from  $T_d = 500 \text{ ns}$  to  $T_d = 31.25 \text{ ns}$ , as shown in Fig. 8. The IPI is avoided or unobvious at this time, while the noise energy is decreased greatly because of lowering  $T_d$ . Then, the BER performance is deteriorated with further decreasing of  $T_d$  (i.e., from  $T_d = 31.25 \text{ ns}$  to  $T_d = 10 \text{ ns}$ ). The IPI becomes so severe that the benefit of decreasing the noise energy is inferior to the adverse effect of increasing IPI, especially in the case of higher signal noise ratio (SNR). Thus, there exists an optimal value  $T_d$  responsible for the corresponding to the best BER performance. Considering the delay lines requirements, the optimal  $T_d$  is set as  $15.625 \text{ ns}$  in the following simulations.

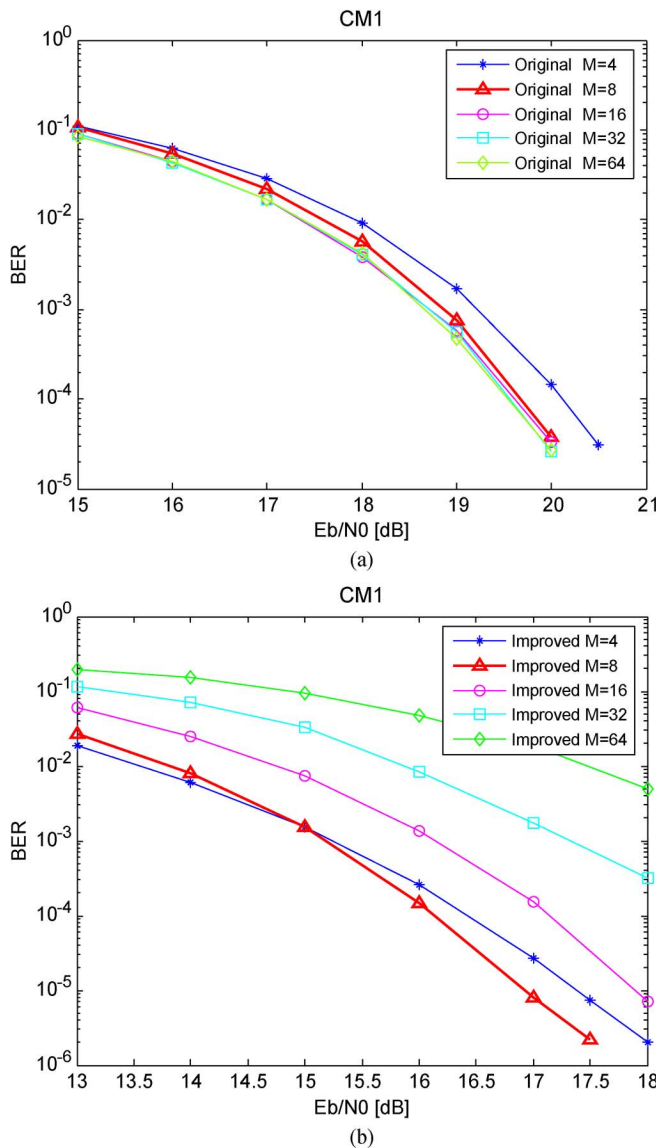


Fig. 9. BER performance of the proposed SIMO FM-DCSK UWB system with different Walsh function orders  $M$ . (a) Original version. (b) Improved version.

### B. Performance of the Original and Improved SIMO FM-DCSK UWB Systems With Different System Parameters

In this subsection, the influences of the order  $M$  of the Walsh function and the receiver antenna number  $N$  to the system performance are considered, in both the original and the improved versions of the SIMO FM-DCSK UWB system.

In the original version based on DC detection, the collected effective signal energy in each receiver antenna is equal to  $(1 - 1/M)E_b$  as shown in (11), which is increased with the increase of  $M$  when the bit energy  $E_b$  is constant. However, some adverse effects are also caused by increasing  $M$ , e.g., more IPI and more noise energy. Besides, the energy of each pulse may become too low to against the noise effect when  $M$  is very large. Consequently, an optimal  $M$  may be sought for the original version of the proposed scheme according to the best BER performance. When  $T_d$  is set to be 15.625 ns (optimized), Fig. 9(a) shows that the BER performance of the original version becomes better as  $M$  is increasing from 4 to 64. But the performance gain is reduced gradually. It can be observed that the

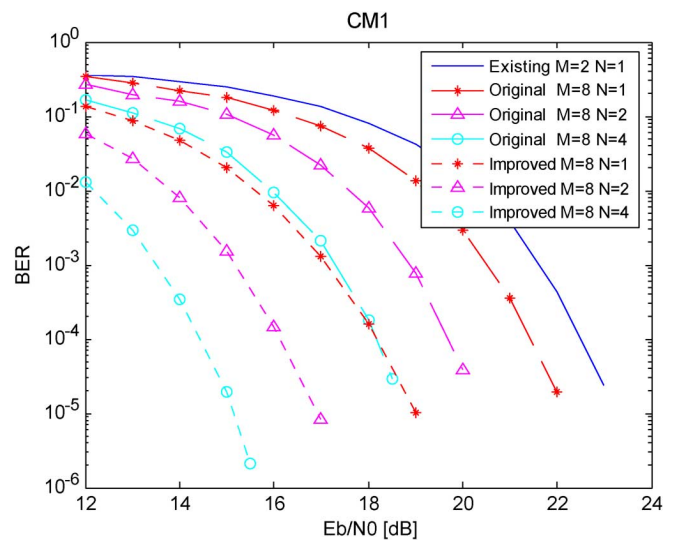


Fig. 10. BER performance comparison between the proposed SIMO FM-DCSK UWB systems with different receiver antenna numbers  $N$  (original version (dashed) and improved version (dotted)) and the existing FM-DCSK UWB system (solid).

performances of the proposed system are close to each other for  $M = 8, 16, 32$  and  $64$ . Since the implement complexity is increased with  $M$ ,  $M = 8$  is considered an optimal value for the original version of the system.

The influence of the order  $M$  on the BER performance is quite different in the improved version. Fig. 9(b) shows that the BER performance of the improved version is not necessarily improved when  $M$  is increased from 4 to 64. And it gets even worse when  $M$  is relatively large (e. g.,  $M = 16, 32$ , and  $64$ ). That is because the duration of the signal-only region (i.e., the integration interval of the receiver detector) becomes long with the increase of  $M$ , as can be seen in Fig. 6(b) and (c). Thus, the increase of the noise energy captured by increasing  $M$  in the improved version is much more than that of the original version.

$M = 8$  is an optimal value in both the original and the improved versions. Next, fixed this value of  $M = 8$  and consider the receiver antenna number  $N$ . Fig. 10 shows the performance of the system with  $N = 1, 2$ , and  $4$ , respectively, given the existing system (i.e.,  $M = 2$  and  $N = 1$ ) for comparison. It can be observed that the BER performance is improved with the increasing of  $N$  and the improved system with  $M = 8$  and  $N = 4$  is better than the original system, at about 8 dB when the BER is  $10^{-4}$ . Certainly, the system complexity is also increased with  $N$ , thus an appropriate value of  $N$  should be determined according to the specific requirements in the application at hand.

### C. Performance of the Proposed Multiaccess Scheme

In this subsection, the BER performance of the proposed multiaccess scheme, based on the pulse cluster version, is examined through simulations with different system parameters. Firstly, the influence of  $M$  on the system performance is considered. As in the single-user case of the improved version,  $T = 1 \mu\text{s}$  and  $T_d = 15.625 \text{ ns}$ , thus the user capability  $C_u$  is equal to 32. Accordingly, the user number  $U$  is set to be 32 in all simulations on the multiaccess scheme, with the receiver antenna  $N = 1$  and  $N = 2$  shown in Fig. 11. Since the GML detection is applied here, the BER performance is improved with the increasing of

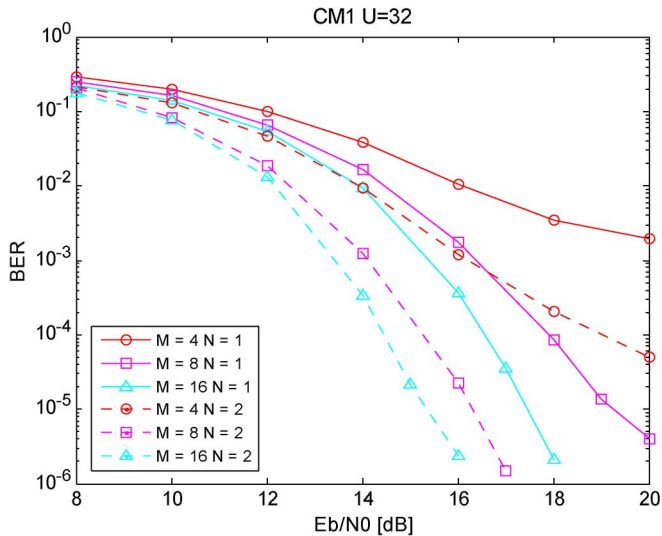


Fig. 11. BER performance of the proposed multiaccess scheme with different Walsh function order  $M$ .

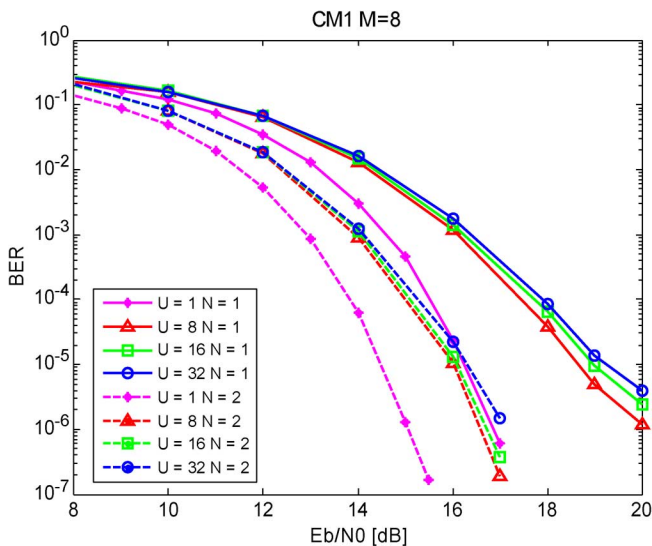


Fig. 12. BER performance of the proposed multiaccess scheme with different user numbers  $U$ .

$M$  due to the  $(M - 1)$  times addition operation which achieves denoising as in the single-user case. This can be seen from both Figs. 11 and 12, when  $M$  is increased from 4 to 8 and 16, respectively.

Now, consider the implement complexity. Set  $M = 8$ , the optimal value for the multiaccess scheme as in the single-user case. It also can be found that the BER performance of the multiusers system is improved with the increase of the receiver antenna number  $N$ . When  $M = 8$ , the 32 user system with  $N = 2$  is better than  $N = 1$  about 2.5 dB when BER is equal to  $10^{-5}$ .

Next, with different user number  $U = 1, 8, 16, 32$ , the BER performance of the proposed multiaccess scheme is shown with the receiver antenna number  $N = 1$  and  $N = 2$  in Fig. 12. As in the above simulations,  $T = 1 \mu\text{s}$ ,  $T_d = 15.625 \text{ ns}$  and the user capability  $C_u$  is set to be 32. In Fig. 12, it is noted that the BER performance of multiusers case is inferior to the single-user case about 3–4 dB, but the BER performance is close when  $U = 8, 16, \text{ and } 32$  no matter in the single receiver antenna and multiple

receiver antenna case. In other words, the performance is not sensitive to the user number  $U$  within the user capability  $C_u$ . Further, one can enhance the user capability by lowering  $T_d$ , e.g.,  $T_d = 7.8125 \text{ ns}$  means  $C_u = 64$ , which may weaken the BER performance as a cost.

Nevertheless, it is no doubt that the proposed scheme has more excellent multiaccess performance comparing with the existing multiaccess scheme for the DCSK/FM-DCSK.

In Figs. 11 and 12, it can be seen that the BER performance of the proposed scheme is always improved with the increase of the receiver antenna  $N$ , no matter what values of  $M$  and  $U$  are. However, considering that the system complexity is increased with  $N$ , i.e.,  $(M - 1)$  delay line units and two correlation integrators are introduced for each additional receiver antenna, an appropriate value  $N_{\text{opt}}$  of the receiver antenna has to be carefully determined according to the specific requirements of the application at hand.

## VI. CONCLUSIONS

An SIMO FM-DCSK UWB system based on a higher order Walsh function has been introduced in this paper to IEEE 802.15.4a low-rate applications. Simulations have shown that the proposed system with either DC or GML detection has significant performance gain as compared with the existing FM-DCSK UWB system, and the system with GML detection outperforms that with DC detection at about 0.5 dB. By trading off BER performance and implementation complexity, the SIMO FM-DCSK UWB system based on DC detection can achieve higher energy efficiency with moderate implementation complexity. Meanwhile, a novel pulse cluster signal structure of the proposed SIMO FM-DCSK UWB system has been presented, not only to reduce the delay lines requirements from hundreds to realizable several nanoseconds, but also to improve the BER performance greatly at about 4–5 dB. Based on the improved signal structure, a new solution to the existing multiaccess scheme utilizing the Walsh function division has also been suggested to resolve the existing implementation obstacle of user capability limited by the order of the Walsh function used. Furthermore, some important parameters have been optimized through simulations, in both cases of single user and multiple users.

With superior BER performance, acceptable delay line requirements and excellent multiaccess capacity, the optimized SIMO FM-DCSK UWB system based on chaotic pulse cluster signals is believed to be a competitive candidate scheme for low-rate and low-power WPAN applications.

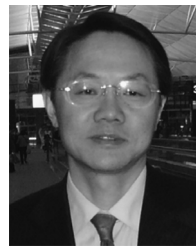
## ACKNOWLEDGMENT

The authors would like to thank Weikai Xu and Shaoyuan Chen for their valuable suggestions.

## REFERENCES

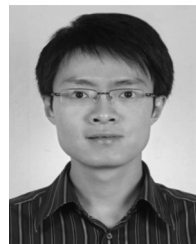
- [1] L. Yang and G. B. Giannakis, "Ultra-wideband communications: An idea whose time has come," *IEEE Signal Process. Mag.*, vol. 21, pp. 26–54, Nov. 2004.
- [2] FCC First Report and Order: In the matter of revision of part 15 of the commission's rules regarding ultra-wideband transmission systems, FCC 02-48, Apr. 2002.

- [3] C. K. Tse and F. C. M. Lau, *Chaos-Based Digital Communication Systems*. New York: Springer-Verlag, 2003.
- [4] J. Pizolato, M. Romero, and L. Goncalves-Neto, "Chaotic communication based on the particle-in-a-box electronic circuit," *IEEE Trans. Circuits Syst. I, Reg. Papers*, vol. 55, no. 4, pp. 1108–1115, May 2008.
- [5] J. R. Piper and J. C. Sprott, "Simple autonomous chaotic circuits," *IEEE Trans. Circuits Syst. II, Exp. Briefs*, vol. 57, no. 9, pp. 730–734, Sep. 2010.
- [6] S.-M. Han, O. Popov, and A. A. Dmitriev, "Flexible chaotic UWB communication system with adjustable channel bandwidth in CMOS technology," *IEEE Trans. Microw. Theory Tech.*, vol. 56, no. 10, pp. 2229–2236, Oct. 2008.
- [7] C. C. Chong and S. K. Yong, "UWB direct chaotic communication technology for low-rate WPAN applications," *IEEE Trans. Veh. Technol.*, vol. 57, no. 3, pp. 1527–1536, May 2008.
- [8] Y. H. Kim, J. H. Kim, and C. C. Chong *et al.*, "Chaotic UWB system," *IEEE 802.15-05-0132-03-004a*, Mar. 2005.
- [9] *Wireless Medium Access Control (MAC) and Physical Layer (PHY) Specifications for Low-Rate Wireless Personal Area Networks (WPANs)*, IEEE Std. 802.15.4a, Aug. 2007.
- [10] Z. Galias and G. M. Maggio, "Quadrature chaos-shift keying: Theory and performance analysis," *IEEE Trans. Circuits Syst. I, Reg. Papers*, vol. 48, no. 12, pp. 1510–1519, Dec. 2001.
- [11] W. M. Tam, F. C. M. Lau, and C. K. Tse, "Generalized correlation-delay-shift-keying scheme for noncoherent chaos-based communication systems," *IEEE Trans. Circuits Syst. I, Reg. Papers*, vol. 53, no. 3, pp. 712–721, Mar. 2006.
- [12] G. Kolumbán, M. P. Kennedy, G. Kis, and Z. Jákó, "FM-DCSK: A novel method for chaotic communications," in *Proc. IEEE Int. Symp. Circuits Syst.*, May 1998, pp. 477–480.
- [13] M. P. Kennedy, G. Kolumbán, G. Kis, and Z. Jákó, "Performance evaluation of FM-DCSK modulation in multipath environments," *IEEE Trans. Circuits Syst. I, Fundam. Theory Appl.*, vol. 47, no. 12, pp. 1702–1711, Dec. 2000.
- [14] L. Ye, G. Chen, and L. Wang, "Essence and advantages of FM-DCSK technique versus conventional spread-spectrum communication methods," *Circ., Syst. Signal Proc.*, vol. 24, no. 5, pp. 657–673, Sep./Oct. 2005.
- [15] L. Wang, C. Zhang, and G. Chen, "Performance of an SIMO FM-DCSK communication system," *IEEE Trans. Circuits Syst. II, Exp. Briefs*, vol. 55, no. 5, pp. 457–461, May 2008.
- [16] G. Kolumbán, "UWB technology: Chaotic communications versus non-coherent impulse radio," in *Proc. 2005 Eur. Conf. Circuit Theory Design*, 2005, pp. 79–82.
- [17] G. Kolumbán, T. Kébesz, and M. Bálint, "Non-coherent UWB impulse radio and FM-DCSK: What makes them different," in *Proc. NDES'06*, 2006, pp. 93–96.
- [18] S. K. Yong, C. C. Chong, and G. Kolumbán, "Non-coherent UWB radio for low-rate WPAN applications: A chaotic approach," *Int. J. Wireless Inf. Netw.*, vol. 14, no. 2, pp. 121–131, Jun. 2007.
- [19] X. Min, W. Xu, L. Wang, and G. Chen, "Promising performance of an FM-DCSK UWB system under indoor environments," *IET Commun.*, vol. 4, no. 2, pp. 125–134, Jan. 2010.
- [20] S. Chen, L. Wang, and G. Chen, "Data-aided timing synchronization for FM-DCSK UWB communication system," *IEEE Trans. Ind. Electron.*, vol. 57, no. 5, pp. 1538–1545, May 2010.
- [21] Y.-L. Chao and R. A. Scholtz, "Ultra-wideband transmitted reference systems," *IEEE Trans. Veh. Technol.*, vol. 54, no. 5, pp. 1556–1569, Sep. 2005.
- [22] K. Gabor, "Performance analysis of chaotic communications systems," Ph.D. dissertation, Dept. Meas. Inf. Syst., Budapest Univ. Technol. Econ., Budapest, Hungary, 2005.
- [23] X. Min, W. Xu, and L. Wang, "An SIMO FM-DCSK UWB scheme for low-rate WPAN applications," in *Proc. 9th Int. Symp. Commun. Inf. Technol.*, Sep. 28–30, 2009, pp. 1157–1160.
- [24] G. Kolumbán, M. P. Kennedy, G. Kis, and Z. Jákó, "Chaotic communications with correlator receivers: Theory and performance limits," *Proc. IEEE*, vol. 90, no. 5, pp. 711–732, May 2002.
- [25] G. Kolumbán, G. Kis, F. C. M. Lau, and C. K. Tse, "Optimum noncoherent FM-DCSK detector: Application of chaotic GML decision rule," in *Proc. ISCAS*, Vancouver, May 23–26, 2004, vol. 4, pp. 597–600.
- [26] G. Kolumbán, F. C. M. Lau, and M. Small, "A new description of chaotic waveform communications: The Fourier analyzer approach," in *Proc. ECCTD'03*, Cracow, Poland, Sep. 1–4, 2003, vol. 3, pp. 241–244.
- [27] S. Gezici, F. Tufvesson, and A. F. Molisch, "On the performance of transmitted-reference impulse radio," in *Proc. IEEE GLOBECOM*, Nov. 2004, pp. 2874–2879.
- [28] M. Casu and G. Durisi, "Implementation aspects of a transmitted reference UWB receiver," *Wireless Commun. Mobile Comput.*, vol. 5, no. 5, pp. 537–549, Aug. 2005.
- [29] F. C. M. Lau, M. M. Yap, C. K. Tse, and S. F. Hao, "A multiple-access technique for differential chaos-shift keying," *IEEE Trans. Circuits Syst. I, Fundam. Theory Appl.*, vol. 49, no. 1, pp. 96–104, Jan. 2002.
- [30] F. C. M. Lau, K. Y. Cheong, and C. K. Tse, "Permutation-based DCSK and multiple-access DCSK systems," *IEEE Trans. Circuits Syst. I, Reg. Papers*, vol. 50, no. 6, pp. 733–742, Jun. 2003.
- [31] H. Li, X. C. Dai, and P. X. Xu, "A CDMA based multiple-access scheme for DCSK," in *Proc. IEEE Int. Symp. Circuits Syst.*, May 2004, pp. 313–316.
- [32] Z. Zhou, T. Zhou, and J. Wang, "Performance of multi-user DCSK communication system over multipath fading channels," in *Proc. IEEE Int. Symp. Circuits Syst.*, May 2007, pp. 2478–2481.
- [33] Y. Shi, Y. Chen, Y. Zhou, and Y. Liu, "An improved scheme for multiple access differential chaos-shifts keying system," in *Proc. IEEE Int. Conf. Circuits Syst. Commun.*, May 2008, pp. 358–361.
- [34] A. F. Molisch, K. Balakrishnan, and C.-C. Chong *et al.*, "IEEE 802.15.4a channel model—Final report Tech. Rep. Doc. IEEE 802.15-04-0662-02-004a", 2005.



**Lin Wang** (S'99–M'03–SM'09) received the B.Sc. degree in mathematics (with first-class honors) from the Chongqing Normal University, Chongqing, China, in 1984, the M.Sc. degree in applied mathematics from the Kunming University of Technology, Kunming, China, in 1988, and the Ph.D degree in electronics engineering from the University of Electronic Science and Technology of China, Chengdu, in 2001.

From 1984 to 1986 he was a Teaching Assistant in Mathematics Department of Chongqing Normal University. From 1989 to 2002 he was a Teaching Assistant, Lecturer, and Associate Professor in Applied Mathematics and Communication Engineering at the Chongqing University of Post and Telecommunication, Chongqing. From 1995 to 1996 he spent one year with the Mathematics Department of the University of New England, Australia. In 2003 he spent three months as visiting researcher in the center of Chaos and Complexity Networks of City University of Hong Kong. Since 2003, he has been full-time Professor and Associate Dean in the School of Information Science and Technology of Xiamen University, Xiamen, China. Recently he has become the editor of *ACTA Electronica Sinica* and Guest Associate Editor of the *International Journal of Bifurcation and Chaos*. He holds 8 patents in the field of physical layer in digital communications and has published over 60 journal and conference papers. His current research interests are in the area of channel coding, chaos modulation, and their applications for wireless communication and storage systems.



**Xin Min** received the B.Sc. degree in electronics engineering from the University of Electronic Science and Technology of China, Chengdu, in 2007 and the M.Sc. degree in communication and information systems from Xiamen University, Xiamen, China, in 2010.

Since 2010, he has worked in the Department of Wireless Networks Performance Research, Huawei Company, Chengdu. His research interests are the research and optimization of performance in the long-term evolution (LTE) communication system.



**Guanrong Chen** (M'87–SM'92–F'97) received the M.Sc. degree in computer science from the Sun Yat-sen University, Guangzhou, China, in 1981 and the Ph.D. degree in applied mathematics from Texas A&M University, College Station, in 1987.

Currently he is a Chair Professor and the Founding Director of the Centre for Chaos and Complex Networks at the City University of Hong Kong, China, prior to which he was a tenured Full Professor at the University of Houston, TX.

Prof. Chen is an ISI Highly Cited Researcher in Engineering. He served and is serving as Chief Editor for the IEEE *Circuits and Systems Magazine* and the *International Journal of Bifurcation and Chaos*, and as Deputy Chief Editor, Advisory Editor, and Associate Editors for several international journals including IEEE TRANSACTIONS ON CIRCUITS AND SYSTEMS, IEEE TRANSACTIONS ON AUTOMATIC CONTROL, and the *International Journal of Circuits Theory and Applications*. He received the 1998 Harden-Simons Prize for the Outstanding Journal Paper Award from the American Society of Engineering Education, the 2001 M. Barry Carlton Best Transactions Paper Award from the IEEE Aerospace and Electronic Systems Society, the 2002 Best Paper Award from the Academy of Science of the Czech Republic, the 2005 Guillemin-Cauer Best Transaction Paper Award from the IEEE Circuits and Systems Society, the 2008 State Natural Science Award of China, and the 2010 Ho-Leung-Ho-Lee Science and Technology Award, China. He is an Honorary Professor at different ranks in some 30 universities worldwide.